CpG-activated Regulatory B-cell Progenitors Alleviate Murine Sclerodermatous Chronic GVHD

Viviane A Agbogan
Institut Necker-Enfants Malades
Pauline Gastineau
Institut Necker-Enfants Malades
Emmanuel Tejerina
Institut Necker-Enfants Malades
Saoussen Karray
Universite de Paris Institut de Recherche Saint-Louis
Flora Zavala (flora.zavala@inserm.fr)
CNRS Délégation Paris B https://orcid.org/0000-0002-2338-6802

Research

Keywords: Chronic graft versus host disease, sclerodermatous graft versus host disease, allogeneic stem cell transplantation, regulatory B-cell progenitors, CpG-proBs, regulatory B-cells, cell therapy, fibrosis

Posted Date: October 5th, 2021

DOI: https://doi.org/10.21203/rs.3.rs-944724/v1

Abstract

Background

Development of chronic Graft Versus Host Disease (cGVHD) represents a major impediment in allogeneic hematopoietic stem cell transplantation (HSCT). This disorder is associated with severe impairment of B-cell homeostasis, regulatory B-cell function and distribution. Conversely, the presence of bone marrow and circulating hematogones is associated with reduced GVHD risks. These findings raised the question whether B-cell progenitors, which provide protection in various autoimmune disease models following activation with the TLR-9 agonist CpG (CpG-proBs), could likewise reduce disease symptoms in a sclerodermatous model of cGVHD.

Methods

Chronic sclerodermatous GVHD was induced in irradiated Balb/c recipients reconstituted with T- and B-cell-depleted bone marrow cells and splenocytes from C57BL/6J donors. CpG-proB-cell progenitors sorted from in vitro CpG-activated bone marrow cells were then adoptively transferred into GVHD recipients. Their effect on disease symptoms, such as diarrhea, skin fibrosis and survival was evaluated in the therapeutic window defined beforehand. Transferred progenitors were analyzed for migration, differentiation and cytokine expression using flow cytofluorimetric methods, which were also used to establish their impact on T-cell cytokine expression and follicular helper/regulatory T-cell ratios (Tfh/Tfr) in peripheral and mesenteric lymph nodes. Skin fibrosis was assessed by histology, identification of infiltrating cells and gene expression profiles of cytokines and molecules involved in the fibrotic process, using qRT-PCR microarrays in all tissue samples.

Results

We found that CpG-proBs, adoptively transferred during the initial phase of disease, reduced the diarrhea score and mostly prevented cutaneous fibrosis. Progenitors migrated to the draining lymph nodes and to the skin where they mainly differentiated into follicular B cells. CpG activation and IFN-γ expression were required for the protective effect, which resulted in reduced $CD4^+$ T-cell-derived production of cytokines critically involved in cGVHD, such as TGF-β, IL-13 and IL-21. Adoptive transfer increased the Tfr/Tfh ratio. Moreover, CpG-proBs privileged the accumulation of IL-10-positive $CD8^+$ T cells, B cells and dendritic cells in the skin.

Conclusion

Our findings support the notion that adoptively transferred CpG-proBs provide an efficient strategy for alleviating sclerodermatous cGVHD either *per se* or as a beneficial adjunct to the HSC graft.

Background

Chronic graft-versus-host disease (cGVHD), a donor T- and B-cell-mediated immune disorder resulting in multi-organ fibrosis and dysfunction, represents a major drawback for long-term effectiveness of allogeneic hematopoietic stem cell transplantation (HSCT) in hematologic malignancies. Efforts to improve immune regulation to prevent this disease have remained challenging. In addition to regulatory T cell deficiencies in both acute and chronic GVHD [1–3], aberrant B cell homeostasis [4], with reduced generation of bone marrow (BM) B lymphoid progenitors [5], low frequencies of naive and memory cells, and a Breg cell defect have recently been described [6, 7]. This led to the hypothesis that tolerogenic B-cell progenitors might play a role in the outcome of HSC transplantation. In accordance with this hypothesis, high numbers of donor BM B-cell progenitors were inversely correlated with the occurrence of GVHD in its acute (aGVHD) [8, 9] or chronic (cGVHD) form [10, 11] in HSC-transplanted patients. More recent studies have shown that their expansion at the time of engraftment heralded less frequent development of severe GVHD and increased mature B-cell counts and IgG levels post-HSCT [12, 13]. Circulating B-cell progenitors have been detected in very low numbers in patients with low-grade GVHD scores [14]. Whether they exhibit any suppressive properties either directly or by promoting the emergence of other regulatory cell types involved in GVHD inhibition remains unknown so far.

We have recently shown in mice that MyD88-dependent activation of BM cells by the Toll-like receptor-9 (TLR-9) agonist CpG-B as well as its injection *in vivo*, induced the emergence within the BM of a B-cell progenitor population, at the pro-B cell stage of differentiation, endowed with potent suppressive properties against autoreactive $CD4^+$ T cells. Importantly, these progenitors migrated into the autoimmune reaction sites and differentiated *in vivo* into several more mature B-cell subsets, which also shared suppressive properties [15–17]. This *in vivo* maturation of the CpG-proBs into suppressive Bregs may account for the long-lasting effect of a single injection of CpG-proBs as well as for their remarkable suppressive potency. Indeed, as few as 60,000 CpG-proBs injected once at the onset of clinical signs were able to provide protection against nonobese type 1 diabetes (T1D) [15] and EAE [16], a murine model of multiple sclerosis.

The efficacy of CpG-proBs in murine autoimmunity models prompted us to examine whether this activated population could likewise provide protection in an allogeneic setting, namely a sclerodermatous model of cGVHD [18] that has also been reported for sharing features of autoimmune inflammation. To this end, we evaluated the effect of CpG-proBs on cGVHD in terms of severity of diarrhea, skin fibrosis and survival. We examined how these cells migrated into diverse sites of the allogeneic response, including mesenteric lymph nodes (mLN), peripheral lymph nodes (pLN) and skin and analyzed their differentiation into more mature B-cell subsets. We further assessed their capacity to modulate the cytokine profile during cGVHD and determined which cytokines were required for protection. Finally, we investigated how the administration of CpG-proBs affected the Tfr/Tfh ratio, which is key in controlling the germinal center (GC) response.

Methods

Mice.

Female Balb/c mice were obtained from Janvier Laboratories (Le Genest Saint Isle, France) and maintained under acidified water upon arrival. Donor cells were from SPF C57BL/6J mice (from Janvier laboratories), congenic CD45.1^{+} C57BL/6J, Actin-GFP KI C57BL/6J, IFN-γ deficient C57BL/6J mice, all raised in our accredited animal facility at Institut Necker Enfants Malades under pathogen-free conditions. All mice were backcrossed for at least ten generations.

Chronic GVHD induction and clinical scoring.

Balb/c mice (female, 10 wk-old) were irradiated at 5.8 Gy in a Faxitron X-Ray irradiator at day 0 and reconstituted at day+1 by i.v. retro-orbital injection with 5 x 10^6 T- and B-cell-depleted BM cells as well as 1 x 10^6 splenocytes from C57BL/6J donors. Clinical evolution of cGVHD was scored over 60-80 days, for survival, diarrhea, weight, posture, mobility and skin damage [18].

T- and B-cell depletion of BM cells.

Donor T- and B-cell-depleted (TBCD) BM cells were isolated by flushing femurs and tibias from donor mice with RPMI 1640. After centrifugation, cells were stained for 15 min with anti-CD3-PE and anti-CD19-PE in PBS, 2% FCS and rat anti-mouse IgG and sheep anti-mouse IgM were added. Depletion was completed with anti-rat and anti-sheep beads, respectively (ThermoFisher Scientific) after 3 passages over a magnet in 5ml tubes. The TBCD-BM fraction contains mainly myeloid, precursor and stem cells.

B-cell progenitor sorting and expansion.

CpG-proB cells were isolated from C57BL/6J BM cell cultures activated with 1 μM CpG-1668 (CpG-B) (Eurogentec, Angers, France) for 17h in low endotoxin-RPMI medium (Fisher Scientific, Illkirch, France) supplemented with 10% (vol/vol) FCS and 1% antibiotics (penicillin and streptomycin). c-kit^{+} cells were magnetically sorted using the Robosep automaton (StemCell Technologies, Grenoble, France) and thereafter stained with appropriately labeled mAbs and sorted by flow cytometry on a BD FACS Aria IIIu cell-sorter as c-kit^{+}Sca-1^{+}B220^{+}PDCA-1^{-}IgM^{-} cells. Electronically sorted B-cell progenitors were cultured on plates at 20,000 cells/ml over OP-9 stromal cells in OPTIMEM medium (Gibco) supplemented with 10% FCS, 1% antibiotics, 0.1% β-mercaptoethanol and 20 ng/ml Flt3L, SCF (Immunotools, Frisoythe, Germany) and IL-7 (Peprotech France, Neuilly-sur-Seine, France), achieving on average a 10-fold expansion of sorted CpG-proBs over 6 days. Expanded CpG-proBs were further stained and electronically sorted as c-kit$^{low/-}$ Sca-1^{+}B220^{+}PDCA-1^{-}IgM^{-} cells before i.v. injection through the retro-orbital sinus.

Recovery of cells from lymph nodes and skin samples.

Inguinal (n=2), axillary and brachial (n=4), cervical (n=2) and mesenteric (n=3) lymph nodes were collected from GVHD controls and CpG-proB recipients, yielding equivalent cell counts in both groups. Skin samples were harvested and digested in RPMI medium (Fisher Scientific, Illkirch, France) supplemented with 1% (vol/vol) FCS, 1% antibiotics (penicillin and streptomycin), 1mg/mL collagenase and 1,000 IU DNase (Sigma-Aldrich, Fleury-Mérogis, France) for 45 min at 37°C.

Flow cytometry analysis of cell subsets and cytokine expression.

To block nonspecific Fc receptor binding, cells were pre-incubated for 10 min at room temperature with FcR blocker 2.4G2 mAb. Cells were then stained with appropriately labeled mAbs against CD4, B220, MHC II, PDCA-1, PDL-1, PDL-2, CD21, IgM, CD93, CD23, CD11b, F4/80 (eBioscience, ThermoFisher Scientific, Montigny-le-Bretonneux, France), c-Kit (CD117) (BioLegend, San Diego, CA), Sca-1 (anti-Ly6A/E), CD40, CD80, CD86, CD11c, CD8 (BD Bioscience/Pharmingen, Le Pont-de-Claix, France), CXCR5 (Sony, Weybridge, Surrey, UK) or GFP (ThermoFisher Scientific). Nuclear Foxp3 expression was measured by FACS analysis as per the manufacturer's instructions (eBioscience, ThermoFisher Scientific). Positive cells were defined using an isotype control antibody. Intra-cytoplasmic cytokine expression was assessed after a 4-h stimulation with PMA (10 ng/ml) plus ionomycin (500 ng/ml) in the presence of Brefeldin A (2 mg/ml), followed by fixation/permeabilization with PFA/saponin and subsequent staining with specific antibodies including PE-labeled anti-TGF-β, PE-labeled anti-IL-27p28, PE-labeled anti-GM-CSF, APC-labeled anti-IL-10, APC-labeled anti–IFN-γ, APC-labelled anti-IL-21 (eBioscience), APC-labeled anti-IL-17 (BD bioscience), FITC-labeled anti-IL-6, PE-labeled anti-IL-13, APC-labeled anti-IL-4 (Sony) and FITC-labeled anti-TNF-α (Biolegend). Positive cells were defined using isotype Ab-stained controls (BD Biosciences and eBioscience). Membrane and intracellular antigen expression was analyzed in a FACS Canto II cytometer (BD Biosciences) using FlowJo software (Treestar, Ashland, OR).

qRT-PCR microarray analysis in skin samples.

Skin samples ($2cm^2$) were collected from the back of GVHD controls or CpG-proB recipients, frozen in liquid nitrogen and stored at -80°C. Frozen tissues were then placed in Qiagen lysis buffer and dissociated using GentleMACS dissociator (Miltenyi Biotec, Paris, France). RNA was extracted with RNeasy Plus Universal mini-Kit (Qiagen, Courtaboeuf, France) following the manufacturer's instructions. The A260/A280 values of all RNA samples ranged from 2.06-2.1. Production of cDNA from 1ng of total extracted RNA was performed using random primers (Invitrogen, ThermoFisher Scientific, Montigny-le Bretonneux, France) and reverse transcriptase superscript II (Life Technologies, Villebon-sur-Yvette, France). qRT-PCR array for measuring the expression of 80 genes of interest (and 8 house-keeping genes), targeting cytokines and fibrosis-related genes, was performed on a custom-made plate (Anygenes, Paris, France) with SYBRGreen, using a qTower2 thermal cycler (Analytic Jena, Jena, Germany). Analysis was performed with Qlucore software (Lund, Sweden). Results are expressed as 2-(delta delta Ct) and gene expression was normalized using the geometrical mean of 6 housekeeping genes. The threshold for the selection of differentially expressed genes was an expression fold-change ≥ 1.4 and a $p \leq 0.05$.

Histology.

Skin sections (4 μm thick) were fixed in 4% paraformaldehyde, embedded in paraffin and stained with H&E. Epidermal thickness was measured on scanned images with NDP.view software (Hamamatsu City, Japan).

Statistics.

Statistical analysis was performed using GraphPad Prism (GraphPad Software, La Jolla, CA). Normality and variance equality were assessed for every data set with Shapiro-Wilk test (for samples with n>5) or D'Agostino-Pearson (for samples with n≤5) and F Test respectively. Survival curves were analyzed with Kaplan-Meier estimates. Disease curves and multiple cytokine production were analyzed using a two-way ANOVA test, with Bonferroni multiple comparison post-test. Cell proportions were analyzed using two-way ANOVA with Bonferroni multiple comparison, Student's *t*-test or one-way ANOVA. Data are shown as mean ± SEM. $P \leq 0.05$ was considered statistically significant.

Results

CpG-proBs protect against cGVHD: Assessment of cellular dose and therapeutic window

After induction, cGVHD went through an initial phase accompanied by diarrhea between day+2 and day+18 followed by a chronic stage from day+20 onwards, characterized by a second bout of diarrhea together with cutaneous manifestations. CpG-proBs were sorted as c-kit^{+}Sca-1^{+}B220^{low}PDCA-1^{-}IgM^{-} cells, as reported before [16] (Supplementary Fig. 1A). A dose of 10^5 CpG-proBs, previously shown to be effective in autoimmune settings, did not significantly reduce the severity of cGVHD, when the adoptive transfer took place the day following reconstitution (Supplementary Fig. 1B). To increase the amount of progenitors available for transfer, CpG-proBs were co-cultured with OP-9 stromal cells for 6 days. After a 10-fold expansion, on average, these progenitors were electronically sorted. They shared a similar phenotype with CpG-proBs that had not been expanded, except for the loss of c-kit expression, presumably resulting from the presence of its ligand SCF in the expansion medium (Supplementary Fig. 1C). When 7.5 x 10^5 CpG-proBs per recipient were injected on day+2 post-irradiation (DPI), they provided significant protection, as assessed by reduced diarrhea and less skin damage but no significant increase in survival compared to controls with cGVHD (Fig. 1). By contrast, the same number of non-activated pro-B cell progenitors freshly sorted from the bone marrow as c-kit^{+}Sca-1^{-}B220^{+}CD24^{hi}CD43^{hi} cells (Supplementary Fig. 1C) and expanded in the same conditions had no such effect (Fig. 1). The same number of CpG-proBs adoptively transferred on day+9 conserved a reduced but still significant protection against disease symptoms, which was lost when injected on day+23 (Fig. 1).

CpG induced a strong upregulation of MHC class II, together with the co-stimulatory molecule CD80, as well as high CD40 expression on proB cell progenitors, thereby improving their capacity to interact with T-cells. There was no significant difference between CpG-proBs and their unstimulated counterpart, in terms of FasL expression, while PDL-1 was upregulated, compared with unstimulated controls, which did not display this molecule at significant levels (Supplementary Fig. 2A). However, the difference between CpG-proBs and proBs became less pronounced after expansion on the OP-9 cell layer. Finally, FACS analysis of PMA+ionomycin-activated proBs and expanded CpG-proBs revealed no significant difference between their cytokine expression profiles (GM-CSF, TNF-α, IL-10 and IFN-γ) (Supplementary Fig. 2B).

CpG-proBs migrate into peripheral organs where they differentiate

We took advantage of CpG-proBs derived from actin-GFP-KI mice to track their migration in recipients. On day+15, $B220^{+}GFP^{+}$ cells, gated as in Fig. 2A, represented 20-30% of all B cells analyzed and were detected exclusively in CpG-proB recipients, in mesenteric (mLN) and peripheral lymph nodes (pLN) as well as in the skin (Fig. 2B). Using a gating strategy based on relative expression of IgM, CD21, CD23 and CD93 [19–21] in all tissues examined, approximately 40% $B220^{+}GFP^{+}$ cells displayed a $CD21^{low}CD23^{+}CD93^{-}IgM^{+}$ phenotype (Fig. 2C, D), similar to follicular B (FoB) cells, previously identified as the major CpG-proB progeny in NOD mice [15].

Cytokines are expressed in the peripheral CpG-proB progeny

Twenty to 80% $B220^{+}GFP^{+}$ cells expressed various cytokines, including IL-10, TGF-β, IFN-γ, GM-CSF, TNF-α and IL-27, compared with only 10-25% positive cells among the non-CpG-proB-derived $B220^{+}GFP^{-}$ population. These observations suggest that the CpG-proB cell progeny is highly activated, especially in mLN, in which $B220^{+}GFP^{+}$ cells expressing these cytokines, notably IL-10 and TGF-β, were more frequent than in their pLN and skin counterpart (Fig. 2E, F).

CpG-proBs modulate cellular distribution and cytokine expression in cGVHD recipients

We analyzed the effect of adoptively transferred CpG-proBs on various recipient cell populations. On day+15, incidence and cell counts of $CD4^{+}$ T cells or $CD4^{+}Foxp3^{+}$ Treg cells were neither significantly different from controls nor did the cytokine expression by $CD4^{+}$ T-cells in mLN and pLN change (Supplementary Fig. 3A, B). On day+25, once the chronic phase initiated, percentages of $CD4^{+}$, $CD4^{+}Foxp3^{+}$ Treg and $CD8^{+}$ T-cells as well as cell counts were not significantly modified (Fig. 3A, B). However the proportion of $CD4^{+}$ T cells generating cytokines, such as TNF-α, TGF-β, IL-21 and IL-13, which are critically involved in chronic GVHD [22], was significantly reduced in mLN from CpG-proB recipients (Fig. 3C), while only IL-13-expressing $CD4^{+}$ T cells were diminished in pLN (Fig. 3D). No significant difference was noted for IL-10 expression in $CD4^{+}$ cells (Fig. 3C, D), while it was slightly but non-significantly enhanced in mLN $CD8^{+}$ T-cells (Fig. 3E).

Adoptive transfer of CpG-proBs increases the Tfr/Tfh ratio

T follicular helper (Tfh) cells, counterbalanced by T follicular regulatory (Tfr) cells, are known to play a key role in the germinal center (GC) reaction taking place in cGVHD [23, 24]. In addition, Bregs have been reported for interacting with both Tfh and Tfr subsets [25, 26]. This led us to examine how CpG-proBs and their progeny affected the balance between these two populations. TFh evaluation on day+15 disclosed no difference between GVHD controls and CpG-proB recipients (Supplementary Fig. 3C). Conversely, on day+25, the ratio between $CD4^{+}CXCR5^{+}Foxp3^{+}$ follicular T regulatory cells (Tfr) and $CD4^{+}CXCR5^{+}Foxp3^{-}$ follicular helper T (Tfh) cells was markedly increased in both mLNs (Fig. 4A) and pLNs (Fig. 4B) of CpG-proB recipients relative to their counterpart in control mice undergoing cGVHD. Moreover, the percentage of Tfh cells expressing IL-10 was increased in mLN, while Tfh cells expressing IL-21 were diminished in

pLN of mice having received CpG-proBs relative to untreated GVHD controls (Fig. 4C, D). Finally, percentages of $CD19^+GL7^+CD38^{low}$ GC B cells did not differ significantly in spleen and mLN (not shown).

The protection against cGVHD by CpG-proBs depends on IFN-γ production

IFN-γ plays a key role in the protective effect of CpG-proBs in autoimmune T1D [15] and EAE [16]. In GVHD mice, CpG-proBs and their migrated progeny expressed IFN-γ at similar levels, whatever the target tissue (Fig. 2E), which prompted us to evaluate its role in the cGVHD model. Using CpG-proBs isolated from IFN-γ-deficient mice, we found that graft recipients displayed exacerbated diarrhea and skin damage, compared with those having received WT CpG-proBs (Fig. 5A). This finding proved the importance of IFN-γ in the protection against cGVHD by CpG-proBs. The progeny of IFN-γ deficient CpG-proBs having migrated to the mLN did not express IFN-γ as expected, but also generated less IL-10, compared to its WT counterpart (Fig. 5B). Moreover, co-culturing peripheral and mesenteric lymph node cells isolated from naive mice with CpG-proBs significantly enhanced IL-10 expression in gated $CD4^+CXCR5^+PD1^+$ Tfh cells, only when the progenitors were competent IFN-γ producers (Fig. 5C).

CpG-proBs reduce fibrosis and regulate gene expression and infiltrates in the skin

GVHD recipients of CpG-proBs developed less alopecia and skin damage (Fig. 6A right) compared with GVHD controls (Fig. 6A left). Histological analysis of H&E-stained skin sections recovered on day+70 revealed 50% reduced epidermal thickness (Fig. 6B), consistent with diminished skin fibrosis. qRT-PCR microarray expression profiles of genes involved in fibrosis and cytokine production (Fig. 6C) established that *Col3a1* as well as of *Pdgfa*, a Col3a1 inducer implicated in fibrosis were downregulated in samples from CpG-proB recipients. The expression of Pdgfa, a known inducer of CXCR4 [27], which attracts fibrocytes to fibrotic tissues [28, 29] was likewise reduced in the skin of CpG-proB recipients. By contrast, thrombospondin-2 (*thsb2*, TSP-2), an anti-angiogenic matricellular protein that improves wound healing [30] was upregulated in CpG-proB recipients. The same applied to *MMP9*, which behaves like a collagenase [31] and can further regulate leukocyte infiltration into inflammatory tissues [32] by inactivating a number of chemoattractants. However, neither total immune cell nor T-cell infiltration was significantly different between GVHD controls and CpG-proB recipients on day+15 or day+42 (Fig. 6D). The enhanced *IL12rb* expression suggested a proTh1 effect of CpG-proBs on skin infiltrates, possibly controlling the deleterious Th2-driven fibrotic process. This conclusion was in keeping with the observed decrease in IL-13 expression by $CD4^+$ T-cells in the lymph nodes. Increased Stat6 expression in CpG-proB recipients (Fig. 6D) was intriguing, knowing that this signal transducer can mediate skin fibrosis [33]. However, this upregulation might result from increased expression of IL-33, which occurs upstream of IL-13 [34]. Of note, IL-33 can substitute for IL-2 as an inducer of tissue $ST2^+$ Treg expansion [35]. Although the proportions of $CD4^+Foxp3^+$ Tregs and $CD4^+IL\text{-}10^+$ Tr1 cells were not significantly increased in skin infiltrates, as measured by FACS analysis (Fig. 7), IL-10-expressing $CD8^+$ T cells, reported for their ST-2 expression and responsiveness to IL-33 [36], markedly accumulated in the skin of CpG-proB recipients, both on day+15 and day+42, while total $CD8^+$ T-cell counts and percentages remained unchanged (Fig. 7).

The proportion of IL-10 producers increased also among the $B220^{+}PDCA\text{-}1^{-}$ B subset as early as day+15, while on day+42, both $B220^{+}PDCA\text{-}1^{-}$ B cells and $CD11c^{+}CD11b^{+}$ dendritic cells expressing IL-10 accumulated (Fig. 7). During cGVHD, macrophages stimulated by Fc immunoglobulin fragments contribute to fibrosis by releasing TGF-β. *Csf1r* was enhanced in the microarray analysis of skin samples from CpG-proB recipients. However, FACS analysis of the skin cell infiltrate revealed that cell counts, percentages as well as IL-10 production by $F4/80^{+}CD11b^{+}$ macrophages remained unchanged on day+42 (Supplementary Figure 4). Moreover, microarray analysis detected no significant difference between *Arg* and *iNOS* expression. In mice, CSF1R is expressed by monocytes/macrophages, but also by conventional and plasmacytoid dendritic cells. However, the observed incremental increase in conventional (Fig. 7) and plasmacytoid dendritic cell percentages and IL-10 expression (Supplementary Fig. 5) did not reach statistical significance. A late accumulation of $csf1r^{+}$ cells in the skin analyzed on day+70, compared to the flow cytometry analysis performed on day+42, cannot be excluded.

Collectively, the analysis of skin samples and infiltrates revealed that the histological effects of CpG-proBs resulting in reduced skin damage, including fibrosis, epidermal thickness and collagen accumulation. These findings correlated with immune tolerance evidenced by enhanced infiltration by IL-10-expressing DCs, $CD8^{+}$ T cells and B cells. The two latter populations were first to accumulate in the skin.

Discussion

Herein, we propose a novel cell therapy based on adoptive transfer of CpG-activated B-cell progenitors in a sclerodermatous model of chronic GVHD. This study was initiated by recent evidence for Breg deficiencies and impaired functions in patients suffering from this disease [3, 7], together with the observation that circulating hematogones and protection against GVHD [8–14] were correlated. These findings warranted further exploration of the regulatory functions of B-cell progenitors in the allogeneic model of cGVHD, expanding our previous studies in experimental models of autoimmune diseases, such as T1D [15] and EAE [16].

A single injection of as few as 7.5×10^{5} CpG-proBs was sufficient to protect against cGVHD, by reducing diarrhea and skin fibrosis within a therapeutic window extending from day+2 to day+9. The effect vanished when these cells were injected on day+23, indicating that they must intervene during the onset of disease to prevent its chronic phase. Protection required around 10-fold higher cell numbers than those needed in the case of organ-specific autoimmune disorders, presumably reflecting the necessity to migrate into the multiple tissues implicated in the allogeneic immune response.

Indeed, CpG-proB progeny was detected in the target sites of cGVHD, including mLN, pLN and skin, as early as day+15, mainly differentiated into Fo B cells, as previously observed in the T1D model of NOD mice [15]. Compared to non-CpG-proB-derived B cells in the same locations, the differentiated CpG-proBs were highly activated, as assessed by a 2-8 fold higher proportion of cells expressing cytokines, such as IFN-γ, GM-CSF, TNF-α, as well as IL-10, TGF-β and IL-27. Among these, IFN-γ production by CpG-proBs and

their progeny proved to be critical for alleviating cGVHD symptoms, particularly skin fibrosis, as previously shown in experimental models of autoimmune diseases, such as T1D [15] and EAE [16].

While CpG-proBs had to be adoptively transferred during the initial phase of GVHD for protection, their effect on the T-cell cytokine profile was observed mostly on day+25, when the expression of $CD4^+$ T-cell-derived cytokines involved in the inflammatory, humoral and fibrotic features of cGVHD, such as TNF-α, IL-21, TGF-β and IL-13, was significantly reduced in mLNs and pLNs. Conversely, as early as day+15, IL-10-expressing B cells and $CD8^+$ T-cells accumulated in the skin of CpG-proB recipients, suggesting an early major contribution of these cells to the protective effect induced by CpG-proBs. In both murine [37, 38] and human [39, 40] GVHDs, IL-10-expressing $CD8^+$ T cells have been reported for their regulatory effects, in particular for reducing collagen deposition in the skin of recipient mice [37]. In the same line of evidence, we found IL-10-expressing dendritic cells accumulating on day+42 in the skin of CpG-proB recipients.

Fo B cells participate in germinal center responses generating long-lived plasma cells and memory B cells. The Tfh/Tfr balance plays a major role in cGVHD, since Tfr cells can inhibit the interplay between Tfh and GC B cells [24–26, 41, 42]. Bregs have been shown to take part in the crosstalk between these subsets in the GC [25, 26, 41]. We found that the CpG-proB progeny belonged mostly to the Fo B phenotype and increased the Tfr/Tfh ratio. IFN-γ was essential for the capacity of the CpG-proB progeny to express IL-10 and enhanced IL-10 expression by Tfh cells. We have previously reported that CpG-proB-derived IFN-γ induced eomesodermin in co-cultured $CD4^+$ T-cells [15]. In turn, EOMES drives IL-10 expression, as shown in Tr1 cells that are protective against GVHD [43]. Whether a similar mechanism takes place in Tfh cells remains to be assessed. Notably, an IL-10 expressing Tfh cell population with suppressive function was identified in chronic viral infection [44] as well as in inflammation associated with aging [45]. Thus, CpG-proBs exert a profound influence on major participants of the GC reaction and IFN-γ production by CpG-proBs is required in both autoimmune and allogeneic settings.

IL-33 expression was enhanced in the microarray qRT-PCR study of skin tissue samples performed at day+70. Even though it has been reported that IL-33, released by epithelial and endothelial cells, induces cutaneous fibrosis, promoting the recruitment of BM-derived eosinophils as well as $CD3^+$ and $F4/80^+$ cell infiltration [46], we observed no accumulation of these cell types. Alternatively, IL-33 has also been described for its capacity to expand and stabilize ST2-expressing Tregs in tissues, thereby favoring tissue remodeling [35, 47]. Treg frequency is inversely correlated with cGVHD in patients [1, 48]. Although we detected no accumulation of $Foxp3^+$ Tregs in CpG-proB recipients compared to cGVHD controls, IL-10^+CD8^+ Tregs were more frequent early in the skin of CpG-proB recipients. These IL-10^+CD8^+ Tregs, which reportedly express ST2 [36], may play a key role in cGVHD recovery.

cGVHD is characterized by the presence of hyperactivated B cells [49]. Conversely, circulating Bregs are less frequent in cGVHD patients and less likely to produce IL-10 than those from healthy donors [3]. In the murine sclerodermatous cGVHD model, reconstitution of donor-derived B10 cells participated in alleviating the disease [50]. Most Breg subsets reported so far for protective effects in cGVHD were

mature B cells. Even cord blood B cells displaying regulatory functions against cGVHD belonged to naive and transitional B-cell subsets [6]. Although an intriguing inverse correlation between BM and circulating B-cell progenitor frequencies and cGVHD severity has been reported, evidence for a regulatory function of B-cell progenitors in cGVHD has been lacking so far. Our findings acquired in a murine experimental model support the notion that innate activation with CpG confers tolerogenic properties to B-cell progenitors that may become instrumental as a protective cell therapy against cGVHD. The fact that these properties remain stable in highly inflammatory settings sheds a new light on Breg ontogeny [51]. Further examination of epigenetic and metabolic changes occurring in these populations may provide further insights into their tolerogenic imprinting.

Conclusion

In this study we provided evidence that adoptive transfer of CpG-proBs at the early phase of cGVHD alleviated disease symptoms, in particular skin fibrosis. Following their migration into lymph nodes and skin, these progenitors depended on IFN-γ production for their protective effect, as previously shown in experimental models of autoimmune diseases. CpG-proB transfer reduced the $CD4^+$ T-cell production of profibrotic cytokines, including TGF-β, IL-21 and IL-13 and enhanced the Tfr/Tfh T-cell ratio in lymph nodes. They also promoted the accumulation of IL-10-producing B-cells, dendritic cells and $CD8^+$ T-cells in the skin (Figure 8). Taken together, our data support a potential benefit of CpG-proBs for cell therapy of cGVHD, either per se or as adjunct to HSC grafts.

Abbreviations

aGVHD, acute GVHD; BM, bone marrow; Bregs, regulatory B cells; cGVHD, chronic GVHD; CpG-proBs, CpG-activated proB cell progenitors; EAE, experimental autoimmune encephalomyelitis; Fo B, follicular B cells; GC, germinal center; HSC, hematopoietic stem cells; HSCT, hematopoietic stem cell transplantation; mLN, mesenteric lymph nodes; pLN, peripheral lymph nodes; T1D, Type 1 diabetes; TBCD-BM, T-and B-cell depleted bone marrow; TFh, follicular helper T cells; TFr, follicular regulatory T cells; TGF-β, Transforming growth factor-beta; Treg, regulatory T cells; SPF, specific pathogen free.

Declarations

Acknowledgments

Authors are indebted to Jérôme Mégret from the flow cytometry platform and Sophie Berissi from the histology platform, SFR Necker, for technical help. They are grateful to Dr Elke Schneider for editorial assistance.

Authors' contributions

V.A.A., P.G., E.T. and F.Z. performed experiments, analyzed data and prepared figures. SK provided expertise in the model, analyzed and discussed data. V.A.A., S.K. and F.Z. wrote the manuscript.

Funding

This work was supported by core funding from CNRS and INSERM. It was also funded by grants to FZ from Agence Nationale de la Recherche (ANR-17-CE17-0008), from Fondation pour la Recherche contre le Cancer (ARC), and from The Secular Society (TSS). VAA was supported by a doctoral fellowship from TSS.

Availability of data and materials

Microarray data are available at GEO under accession number GSE 182025 [https://www.ncbi.nlm.nih.gov/geo/query/acc.cgi?acc=GSE182025]. Other data that support the findings of this study are available from the corresponding author upon reasonable request.

Consent for publication

Not applicable.

Competing interests

The authors have no conflict of interest to declare.

References

1. Zorn E, Kim HT, Lee SJ, Floyd BH, Litsa D, Arumugarajah S, et al. Reduced frequency of FOXP3+ CD4+CD25+ regulatory T cells in patients with chronic graft-versus-host disease. Blood. 2005;106:2903–2911. doi:10.1182/blood-2005-03-1257.
2. Matsuoka K, Kim HT, McDonough S, Bascug G, Warshauer B, Koreth J, et al. Altered regulatory T cell homeostasis in patients with CD4+ lymphopenia following allogeneic hematopoietic stem cell transplantation. J Clin Invest. 2010;120:1479–1493. doi:10.1172/JCI41072.
3. Khoder A, Sarvaria A, Alsuliman A, Chew C, Sekine T, Cooper N, et al. Regulatory B cells are enriched within the IgM memory and transitional subsets in healthy donors but are deficient in chronic GVHD. Blood. 2014;124:2034–2045. doi:10.1182/blood-2014-04-571125.
4. Sarantopoulos S, Stevenson KE, Kim HT, Cutler CS, Bhuiya NS, Schowalter M, et al. Altered B-cell homeostasis and excess BAFF in human chronic graft-versus-host disease. Blood. 2009;113:3865–3874. doi:10.1182/blood-2008-09-177840.
5. Kolupaev OV, Dant TA, Bommiasamy H, Bruce DW, Fowler KA, Tilley SL, et al. Impaired bone marrow B-cell development in mice with a bronchiolitis obliterans model of cGVHD. Blood Adv. 2018;2:2307–2319. doi:10.1182/bloodadvances.2017014977.
6. Sarvaria A, Basar R, Mehta RS, Shaim H, Muftuoglu M, Khoder A, et al. IL-10+ regulatory B cells are enriched in cord blood and may protect against cGVHD after cord blood transplantation. Blood. 2016;128:1346–1361. doi:10.1182/blood-2016-01-695122.

7. de Masson A, Bouaziz J-D, Le Buanec H, Robin M, O'Meara A, Parquet N, et al. CD24(hi)CD27^{+} and plasmablast-like regulatory B cells in human chronic graft-versus-host disease. Blood. 2015;125:1830–1839. doi:10.1182/blood-2014-09-599159.
8. Ishio T, Sugita J, Tateno T, Hidaka D, Hayase E, Shiratori S, et al. Hematogones predict better outcome in allogeneic hematopoietic stem cell transplantation irrespective of graft sources. Biol Blood Marrow Transplant. 2018;24:1990–1996. doi:10.1016/j.bbmt.2018.06.011.
9. Michonneau D, Peffault de Latour R, Porcher R, Robin M, Benbunan M, Rocha V, et al. Influence of bone marrow graft B lymphocyte subsets on outcome after HLA-identical sibling transplants. Br J Haematol. 2009;145:107–114. doi:10.1111/j.1365-2141.2008.07574.x.
10. Sarantopoulos S, Stevenson KE, Kim HT, Washel WS, Bhuiya NS, Cutler CS, et al. Recovery of B-cell homeostasis after rituximab in chronic graft-versus-host disease. Blood. 2011;117:2275–2283. doi:10.1182/blood-2010-10-307819.
11. Fedoriw Y, Samulski TD, Deal AM, Dunphy CH, Sharf A, Shea TC, et al. Bone marrow B cell precursor number after allogeneic stem cell transplantation and GVHD development. Biol Blood Marrow Transplant. 2012;18:968–973. doi:10.1016/j.bbmt.2012.03.005.
12. Shima T, Miyamoto T, Kikushige Y, Mori Y, Kamezaki K, Takase K, et al. Quantitation of hematogones at the time of engraftment is a useful prognostic indicator in allogeneic hematopoietic stem cell transplantation. Blood. 2013;121:840–848. doi:10.1182/blood-2012-02-409607.
13. Doki N, Haraguchi K, Hagino T, Igarashi A, Najima Y, Kobayashi T, et al. Clinical impact of hematogones on outcomes of allogeneic hematopoietic stem cell transplantation. Ann Hematol. 2015;94:2055–2060. doi:10.1007/s00277-015-2492-y.
14. Glauzy S, André-Schmutz I, Larghero J, Ezine S, Peffault de Latour R, Moins-Teisserenc H, et al. CXCR4-related increase of circulating human lymphoid progenitors after allogeneic hematopoietic stem cell transplantation. PLoS One. 2014;9:e91492. doi:10.1371/journal.pone.0091492.
15. Montandon R, Korniotis S, Layseca-Espinosa E, Gras C, Mégret J, Ezine S, et al. Innate pro-B-cell progenitors protect against type 1 diabetes by regulating autoimmune effector T cells. Proc Natl Acad Sci USA. 2013;110:E2199–208. doi:10.1073/pnas.1222446110.
16. Korniotis S, Gras C, Letscher H, Montandon R, Mégret J, Siegert S, et al. Treatment of ongoing autoimmune encephalomyelitis with activated B-cell progenitors maturing into regulatory B cells. Nat Commun. 2016;7:12134. doi:10.1038/ncomms12134.
17. Zavala F, Korniotis S, Montandon R. Characterization and Immunoregulatory Properties of Innate Pro-B-Cell Progenitors. Methods Mol Biol. 2016;1371:79–88. doi:10.1007/978-1-4939-3139-2_5.
18. Wu T, Young JS, Johnston H, Ni X, Deng R, Racine J, et al. Thymic damage, impaired negative selection, and development of chronic graft-versus-host disease caused by donor CD4+ and CD8+ T cells. J Immunol. 2013;191:488–499. doi:10.4049/jimmunol.1300657.
19. Allman D, Lindsley RC, DeMuth W, Rudd K, Shinton SA, Hardy RR. Resolution of three nonproliferative immature splenic B cell subsets reveals multiple selection points during peripheral B cell maturation. J Immunol. 2001;167:6834–6840. doi:10.4049/jimmunol.167.12.6834.

20. Basu S, Ray A, Dittel BN. Cannabinoid receptor 2 is critical for the homing and retention of marginal zone B lineage cells and for efficient T-independent immune responses. J Immunol. 2011;187:5720–5732. doi:10.4049/jimmunol.1102195.
21. Ray A, Khalil MI, Pulakanti KL, Burns RT, Gurski CJ, Basu S, et al. Mature IgDlow/- B cells maintain tolerance by promoting regulatory T cell homeostasis. Nat Commun. 2019;10:190. doi:10.1038/s41467-018-08122-9.
22. MacDonald KP, Blazar BR, Hill GR. Cytokine mediators of chronic graft-versus-host disease. J Clin Invest. 2017;127:2452–2463. doi:10.1172/JCI90593.
23. Srinivasan M, Flynn R, Price A, Ranger A, Browning JL, Taylor PA, et al. Donor B-cell alloantibody deposition and germinal center formation are required for the development of murine chronic GVHD and bronchiolitis obliterans. Blood. 2012;119:1570–1580. doi:10.1182/blood-2011-07-364414.
24. Flynn R, Du J, Veenstra RG, Reichenbach DK, Panoskaltsis-Mortari A, Taylor PA, et al. Increased T follicular helper cells and germinal center B cells are required for cGVHD and bronchiolitis obliterans. Blood. 2014;123:3988–3998. doi:10.1182/blood-2014-03-562231.
25. Ding T, Su R, Wu R, Xue H, Wang Y, Su R, et al. Frontiers of autoantibodies in autoimmune disorders: crosstalk between tfh/tfr and regulatory B cells. Front Immunol. 2021;12:641013. doi:10.3389/fimmu.2021.641013.
26. Achour A, Simon Q, Mohr A, Séité J-F, Youinou P, Bendaoud B, et al. Human regulatory B cells control the TFH cell response. J Allergy Clin Immunol. 2017;140:215–222. doi:10.1016/j.jaci.2016.09.042.
27. Andrae J, Gallini R, Betsholtz C. Role of platelet-derived growth factors in physiology and medicine. Genes Dev. 2008;22:1276–1312. doi:10.1101/gad.1653708.
28. Shin JU, Kim SH, Kim H, Noh JY, Jin S, Park CO, et al. TSLP Is a Potential Initiator of Collagen Synthesis and an Activator of CXCR4/SDF-1 Axis in Keloid Pathogenesis. J Invest Dermatol. 2016;136:507–515. doi:10.1016/j.jid.2015.11.008.
29. Mehrad B, Burdick MD, Strieter RM. Fibrocyte CXCR4 regulation as a therapeutic target in pulmonary fibrosis. Int J Biochem Cell Biol. 2009;41:1708–1718. doi:10.1016/j.biocel.2009.02.020.
30. Kyriakides TR, Maclauchlan S. The role of thrombospondins in wound healing, ischemia, and the foreign body reaction. J Cell Commun Signal. 2009;3:215–225. doi:10.1007/s12079-009-0077-z.
31. Bigg HF, Rowan AD, Barker MD, Cawston TE. Activity of matrix metalloproteinase-9 against native collagen types I and III. FEBS J. 2007;274:1246–1255. doi:10.1111/j.1742-4658.2007.05669.x.
32. Greenlee KJ, Corry DB, Engler DA, Matsunami RK, Tessier P, Cook RG, et al. Proteomic identification of in vivo substrates for matrix metalloproteinases 2 and 9 reveals a mechanism for resolution of inflammation. J Immunol. 2006;177:7312–7321.
33. O'Reilly S. Role of interleukin-13 in fibrosis, particularly systemic sclerosis. Biofactors. 2013;39:593–596. doi:10.1002/biof.1117.
34. Rostan O, Arshad MI, Piquet-Pellorce C, Robert-Gangneux F, Gangneux J-P, Samson M. Crucial and diverse role of IL-33/ST2 axis in infectious diseases. Infect Immun. 2015;83:1738–1748. doi:10.1128/IAI.02908-14.

35. Alvarez F, Fritz JH, Piccirillo CA. Pleiotropic Effects of IL-33 on CD4+ T Cell Differentiation and Effector Functions. Front Immunol. 2019;10:522. doi:10.3389/fimmu.2019.00522.
36. Yang Q, Li G, Zhu Y, Liu L, Chen E, Turnquist H, et al. IL-33 synergizes with TCR and IL-12 signaling to promote the effector function of CD8+ T cells. Eur J Immunol. 2011;41:3351–3360. doi:10.1002/eji.201141629.
37. Iamsawat S, Tian L, Daenthanasanmak A, Wu Y, Nguyen HD, Bastian D, et al. Vitamin C stabilizes CD8+ iTregs and enhances their therapeutic potential in controlling murine GVHD and leukemia relapse. Blood Adv. 2019;3:4187–4201. doi:10.1182/bloodadvances.2019000531.
38. Beres AJ, Haribhai D, Chadwick AC, Gonyo PJ, Williams CB, Drobyski WR. CD8+ Foxp3+ regulatory T cells are induced during graft-versus-host disease and mitigate disease severity. J Immunol. 2012;189:464–474. doi:10.4049/jimmunol.1200886.
39. Alhaj Hussen K, Michonneau D, Biajoux V, Keita S, Dubouchet L, Nelson E, et al. CD4+CD8+ T-Lymphocytes in Xenogeneic and Human Graft-versus-Host Disease. Front Immunol. 2020;11:579776. doi:10.3389/fimmu.2020.579776.
40. Xystrakis E, Dejean AS, Bernard I, Druet P, Liblau R, Gonzalez-Dunia D, et al. Identification of a novel natural regulatory CD8 T-cell subset and analysis of its mechanism of regulation. Blood. 2004;104:3294–3301. doi:10.1182/blood-2004-03-1214.
41. Lal G, Kulkarni N, Nakayama Y, Singh AK, Sethi A, Burrell BE, et al. IL-10 from marginal zone precursor B cells controls the differentiation of Th17, Tfh and Tfr cells in transplantation tolerance. Immunol Lett. 2016;170:52–63. doi:10.1016/j.imlet.2016.01.002.
42. Forcade E, Kim HT, Cutler C, Wang K, Alho AC, Nikiforow S, et al. Circulating T follicular helper cells with increased function during chronic graft-versus-host disease. Blood. 2016;127:2489–2497. doi:10.1182/blood-2015-12-688895.
43. Zhang P, Lee JS, Gartlan KH, Schuster IS, Comerford I, Varelias A, et al. Eomesodermin promotes the development of type 1 regulatory T (TR1) cells. Sci Immunol. 2017;2. doi:10.1126/sciimmunol.aah7152.
44. Xin G, Zander R, Schauder DM, Chen Y, Weinstein JS, Drobyski WR, et al. Single-cell RNA sequencing unveils an IL-10-producing helper subset that sustains humoral immunity during persistent infection. Nat Commun. 2018;9:5037. doi:10.1038/s41467-018-07492-4.
45. Almanan M, Raynor J, Ogunsulire I, Malyshkina A, Mukherjee S, Hummel SA, et al. IL-10-producing Tfh cells accumulate with age and link inflammation with age-related immune suppression. Sci Adv. 2020;6:eabb0806. doi:10.1126/sciadv.abb0806.
46. Rankin AL, Mumm JB, Murphy E, Turner S, Yu N, McClanahan TK, et al. IL-33 induces IL-13-dependent cutaneous fibrosis. J Immunol. 2010;184:1526–1535. doi:10.4049/jimmunol.0903306.
47. Molofsky AB, Savage AK, Locksley RM. Interleukin-33 in Tissue Homeostasis, Injury, and Inflammation. Immunity. 2015;42:1005–1019. doi:10.1016/j.immuni.2015.06.006.
48. Alho AC, Kim HT, Chammas MJ, Reynolds CG, Matos TR, Forcade E, et al. Unbalanced recovery of regulatory and effector T cells after allogeneic stem cell transplantation contributes to chronic GVHD.

Blood. 2016;127:646–657. doi:10.1182/blood-2015-10-672345.

49. McManigle W, Youssef A, Sarantopoulos S. B cells in chronic graft-versus-host disease. Hum Immunol. 2019;80:393–399. doi:10.1016/j.humimm.2019.03.003.
50. Le Huu D, Matsushita T, Jin G, Hamaguchi Y, Hasegawa M, Takehara K, et al. Donor-derived regulatory B cells are important for suppression of murine sclerodermatous chronic graft-versus-host disease. Blood. 2013;121:3274–3283. doi:10.1182/blood-2012-11-465658.
51. Rosser EC, Mauri C. Regulatory B cells: origin, phenotype, and function. Immunity. 2015;42:607–612. doi:10.1016/j.immuni.2015.04.005.

Supplementary Figure

Supplementary Figure 5 is not available with this version.

Figures

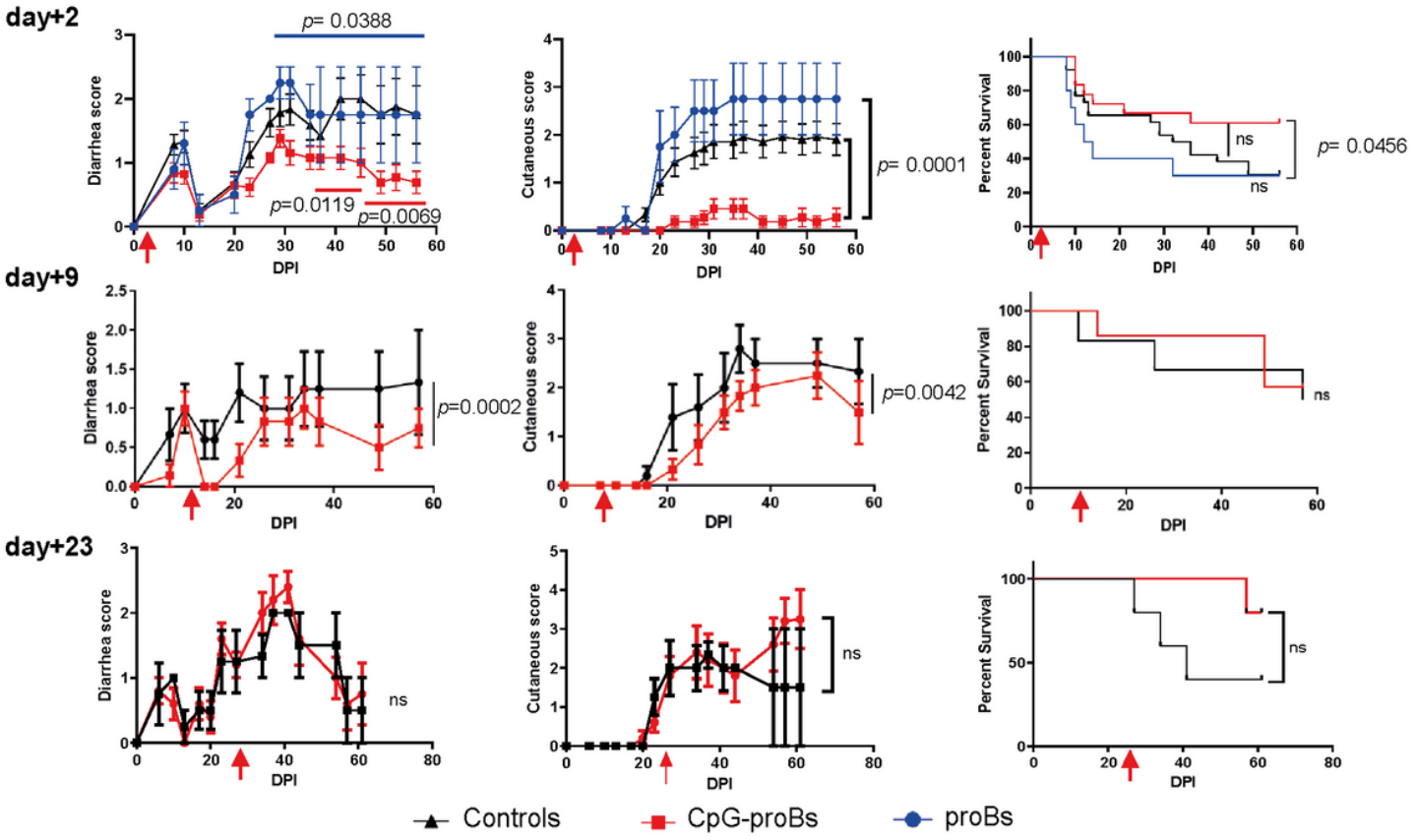

Figure 1

Effect of adoptively transferred CpG-proBs on chronic GVHD symptoms. Balb/c recipients irradiated at 5.8 Gy on day-0, were reconstituted on day+1 with T- and B-cell depleted BM cells (5x106 cells) and splenocytes (1 x 106 cells) from C57BL/6J donors. CpG-proBs (7.5 x 105cells) or proBs prepared from C57BL/6J donors and expanded in co-culture with OP-9 stromal cells were adoptively transferred on

day+2, day+9 or day+23 post-irradiation (DPI) as indicated. Diarrhea, cutaneous scores and survival are shown over a period of 60-80 days. Results are expressed as means ± SEM. Adoptive transfer was performed on day+2 in GVHD control mice (N=30, black line), CpG-proB recipients (N=19, red line), proB recipients (N=10, blue line); on day+9, in GVHD controls (N=6, black line), CpG-proB recipients (N=7, red line); on day+23, in GVHD controls (N=7, black line) and CpG-proB recipients (N=6, red line). Statistical analysis was performed with two-way ANOVA with Bonferroni post-tests for diarrhea score and cutaneous score and Kaplan-Meier estimates for survival; p values as indicated; ns=non significant.

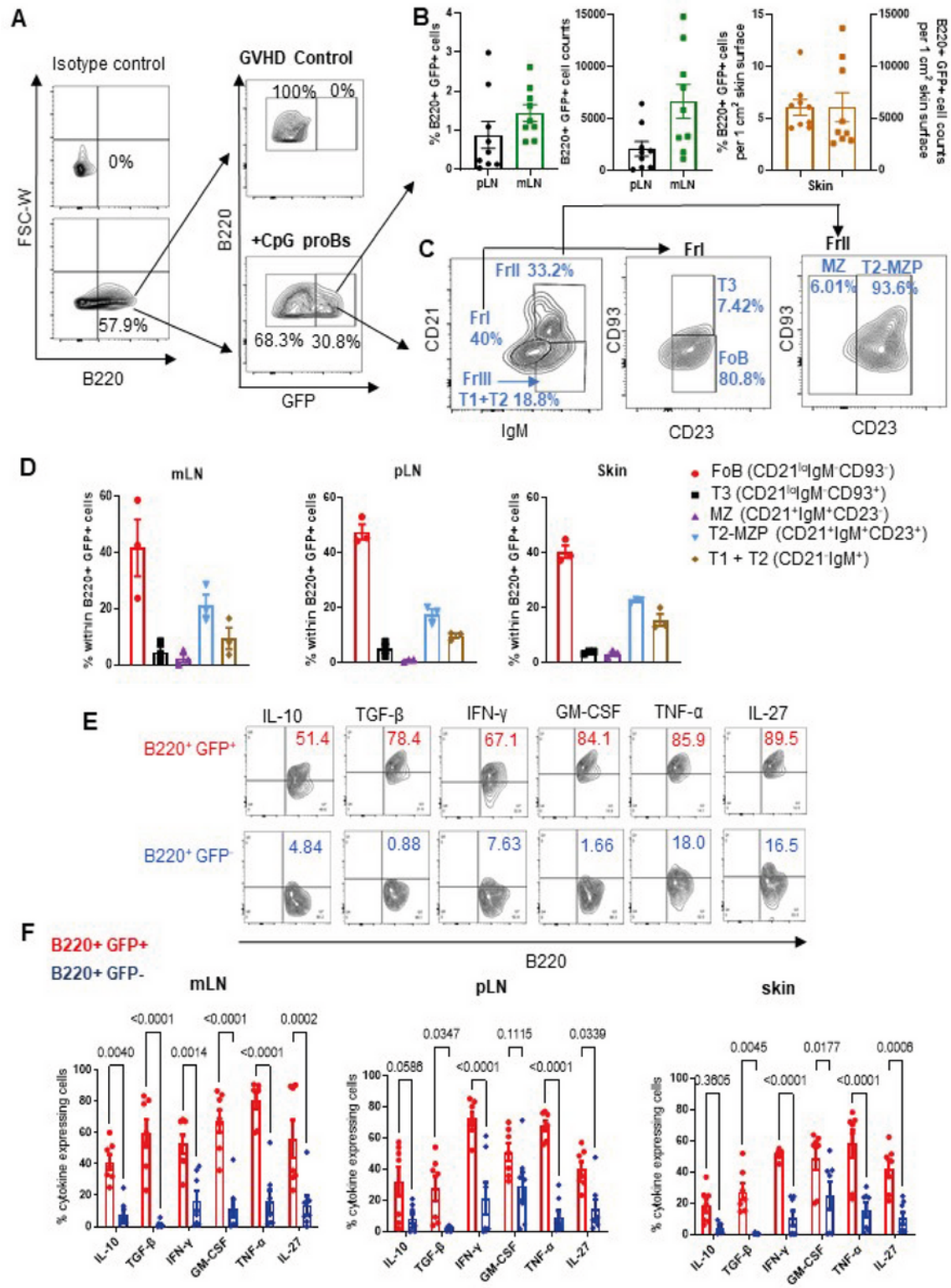

Figure 2

Migration, differentiation and cytokine expression of CpG-proBs in cGVHD mice. CpG-proBs, isolated from the BM of actin-GFP-KI C57BL/6J donors, were adoptively transferred on day+2 post-irradiation. (A) Gating procedure of B220+ GFP+ cells, shown on day+15 in mesenteric lymph nodes (mLN), in controls with GVHD and in CpG-proB recipients, isotype antibody controls being used to define positivity. (B) The migration of B220+GFP+ cells was traced and analyzed by FACS on day+15 in peripheral and mesenteric lymph nodes (pLN), mLN) and skin. Indicated are percentages of B220+GFP+ cells among all recovered cells. In the skin, percentages and counts of B220+GFP+ cells are indicated per 1 cm2 of skin surface. (C, D) Differentiation of CpG-proBs (C) and phenotype of the B220+GFP+ progeny assessed on day+15 in mLN. Isotype antibody controls were used to define positivity. The various B-cell subfractions were defined as FoB (CD21loIgM-CD93-), T3 (CD21loIgM-CD93+), MZ (CD21+IgM+CD23-), T2-MZP (CD21+IgM+CD23+) and T1+T2 (CD21-IgM+) cells. (D) CpG-proB differentiation on day+15 in mLN, pLN and skin. (E, F) Cytokine expression by the CpG-proB progeny on day+15. (E) FACS profiles of cytokine (IL-10, TGF-β, IFN-γ, GM-CSF, TNF-α and IL-27) expression by CpG-proB-derived B220+GFP+ and non-CpG-proB-derived B220+GFP- cells in the mLN. (F) Percent cytokine expressing B220+GFP+ (red) and B220+GFP- (blue) cells in mLN, pLN and skin. Statistical analysis was performed with two-way ANOVA with Bonferroni multiple comparisons. (B, D, F) Results are expressed as mean ± SEM of 3-9 mice per group.

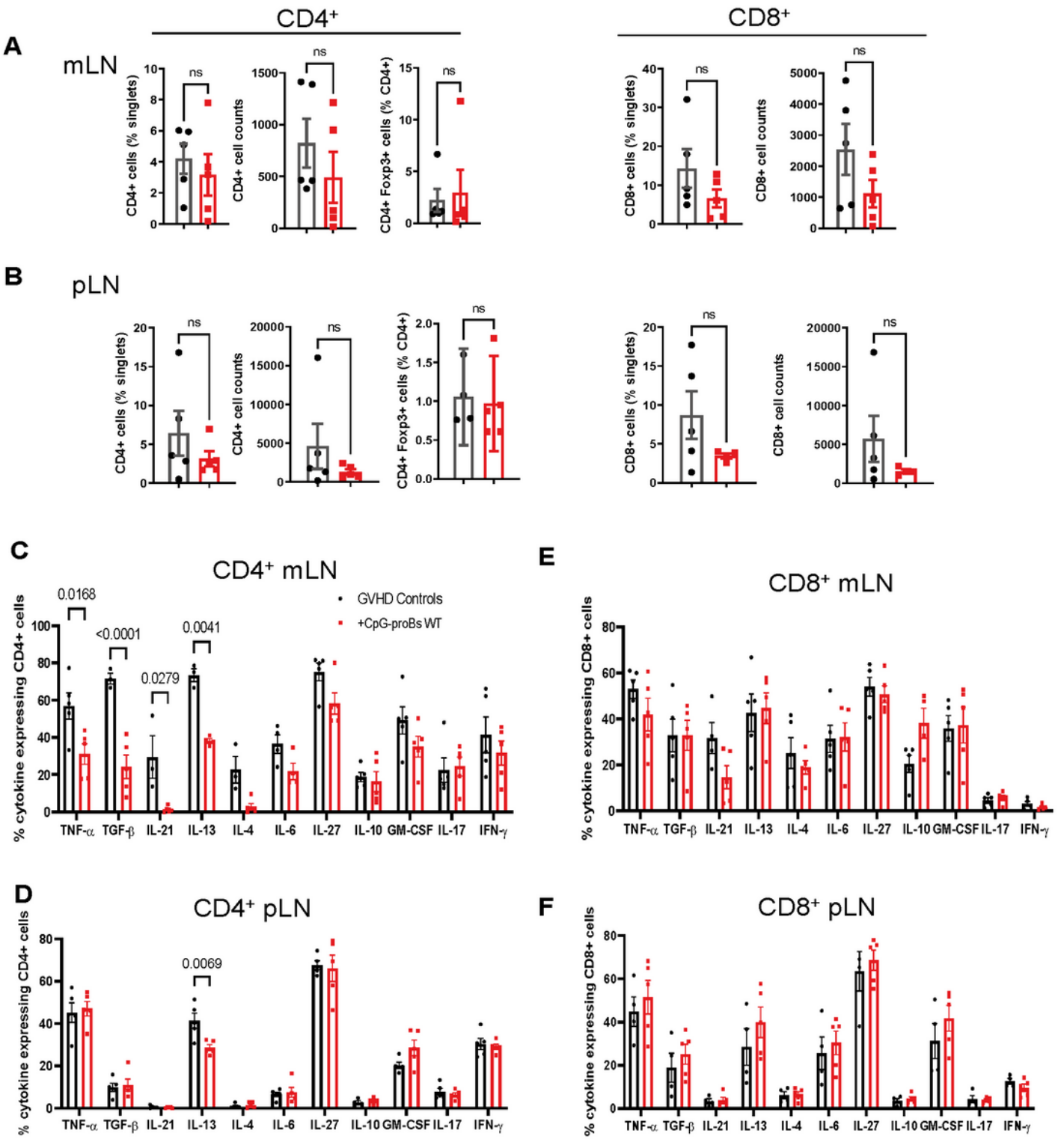

Figure 3

T-cell subset analysis in mLN and pLN of CpG-proB recipients and cGVHD controls. (A, B) Quantification by FACS analysis on day+25 of CD4+, CD8+ (% and cell counts) and CD4+Foxp3+ (%) in mLN (A) and pLN (B) of cGVHD controls (black) and CpG-proB recipients (red). (C, D) Cytokine expression by CD4+ T cells in mLN (C) and pLN (D) of cGVHD controls (black) and CpG-proB recipients (red). Data are expressed as means ± SEM of 5 mice per group. Statistical analysis was performed with unpaired

Students't- test (A, B) and two-way ANOVA with Bonferroni multiple comparisons (C, D). p values as indicated, n.s., non significant.

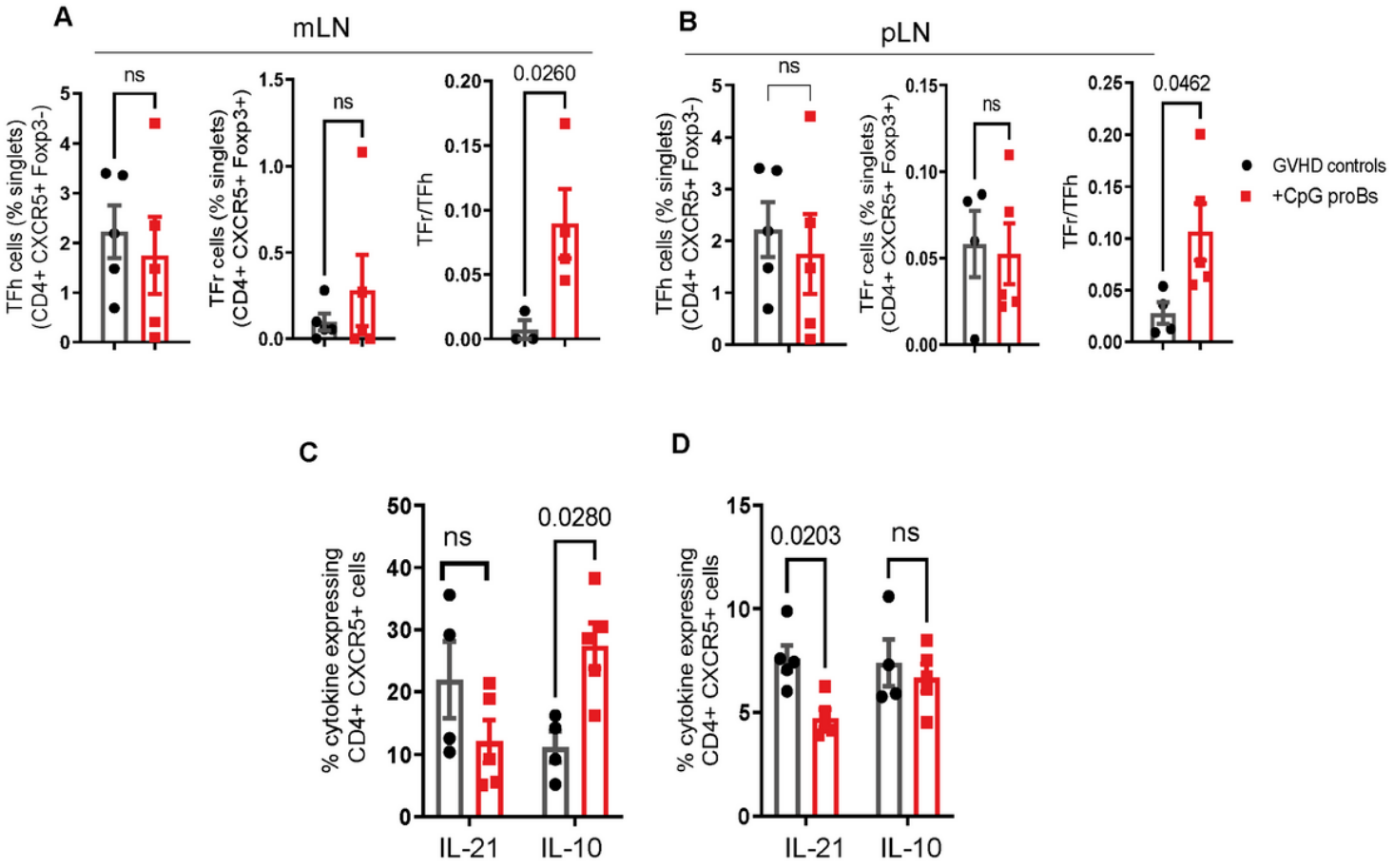

Figure 4

Follicular T-cell (Tf) analysis. (A, B) Percentages and counts of Tfh (CD4+CXCR5+Foxp3-) and Tfr (CD4+CXCR5+Foxp3+) cells as well as Tfr/Tfh ratios on day+25 in mLN (A) and pLN (B) of mice, either CpG-proB recipients (red) or GVHD controls (black). (C, D) Cytokine expression by CD4+CXCR5+ cells. Percent IL-21- and IL-10-expressing cells in mLN (C) and pLN (D) of cGVHD controls (black) and CpG-proB recipients (red). Results are expressed as means ± SEM from 5 mice per group. Statistical analysis was performed with unpaired Students't- test (A, B) and two-way ANOVA with Bonferroni multiple comparisons (C, D). p values as indicated, ns= non significant.

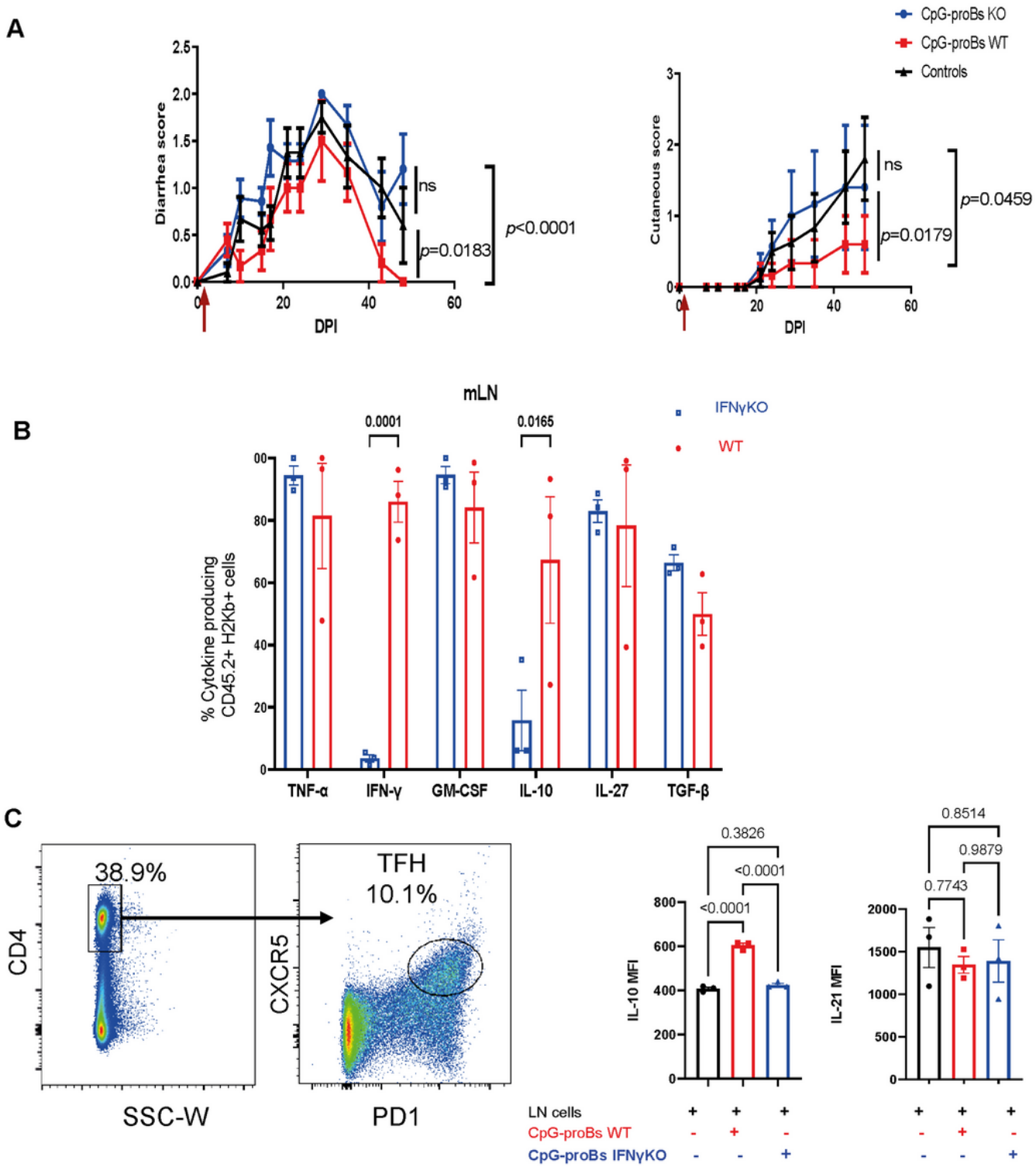

Figure 5

Role of IFN-γ in the protective properties of CpG-proBs against cGVHD. CpG-proBs were prepared from either WT or IFN-γ deficient C57BL/6J donors and adoptively transferred (7.5 x 105 cells/recipient) on day+2 post-irradiation (DPI). (A) Diarrhea and cutaneous scores of cGVHD controls (black, n=10), WT CpG-proB recipients (red, n=9) and IFN-γ deficient CpG-proBs (blue, n=9). Statistical analysis was performed with two-way ANOVA with Bonferroni multiple comparisons for diarrhea and cutaneous

scores. Results are expressed as means ± SEM. P values as indicated. ns= non significant. (B) CpG-proB progeny, derived from either WT (red) or IFN-γ deficient (blue) C57BL/6J CpG-proBs, was gated as CD45.2+ H2Kb+ cells in mLN of cGVHD Balb/c (H2Kd) recipients of CD45.1+ TBCD-BM and splenocytes from CD45.1+C57BL/6J donors and their cytokine expression analyzed as in Figure 2E on day+15 after adoptive transfer. (C) Lymph node cells from naive C57BL/6J mice were co-cultured at a 1:1 ratio with CpG-proBs at 5 x 105 cells/ml for 3 days in RMPI 1640 medium, 10% FCS, 1% antibiotics, 0.1% β-mercaptoethanol in the presence of anti-CD3 (200 ng/ml) and analyzed by FACS for IL-10 and IL-21 expression in gated CD4+CXCR5+ Tfh cells. Statistical analysis was performed with one-way ANOVA for B and C. Results are expressed as means ± SEM. p values as indicated.

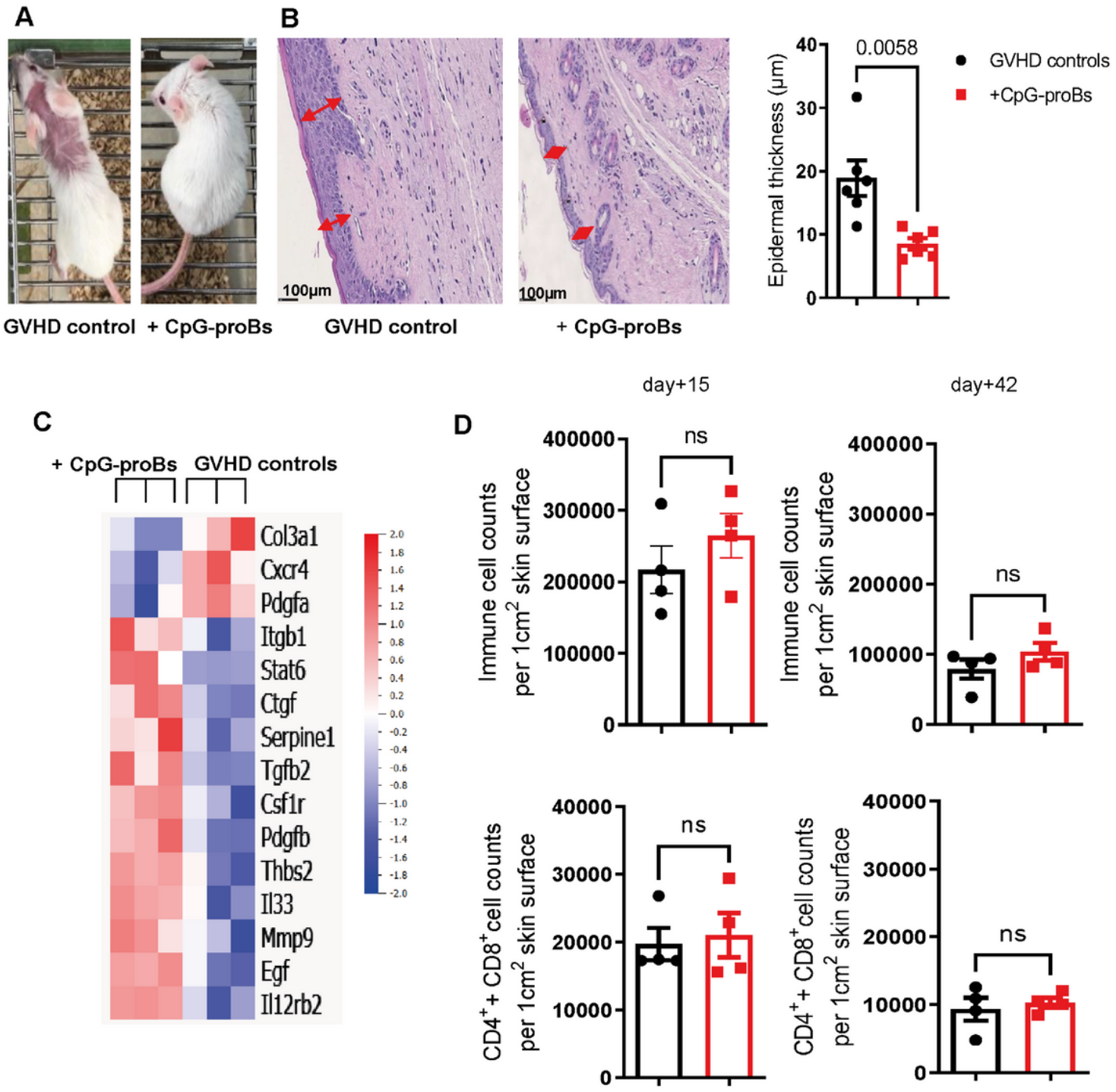

Figure 6

Analysis of skin histological modifications, gene expression and cellular infiltrate in cGVHD controls versus CpG-proB recipients. (A) CpG-proB recipients were mostly protected from alopecia and skin damage induced by cGVHD in Balb/c recipients. Picture of one representative mouse per group. (B) H&E staining of representative skin sections in GVHD controls versus CpG-proB recipients. Scale bar = 100 µm. Red arrows indicate the epidermal thickness. Forty measures were taken per skin section. Right:

Histogram representation of epidermal thickness in GVHD controls (black) and CpG-proB recipients (red). Results are expressed as means ± SEM from 6 mice/group. p value as indicated. Analysis was performed with unpaired Student's t-test. (C) Heatmap showing significant fold-change expression of genes as measured by qRT-PCR microarray in skin fragments (2 cm2) isolated from GVHD controls (right) and CpG-proB recipients (left). N =3 animals per group. Analysis was performed with Qlucore. Genes showing ≥1.4 expression fold change with p≤0.05 were considered significant. Right: Color scale of positive and negative fold-change gene expression. (D) Flow cytometry analysis on day+15 and day+42 of total immune cell infiltrates as well as T-cell (CD4+ and CD8+) infiltrates in skin samples of cGVHD controls (black) and CpG-proB recipients (red). Results are expressed as means ± SEM from 4 mice per group. Statistical analysis performed with unpaired Student's t-test, ns, non significant, p values as indicated.

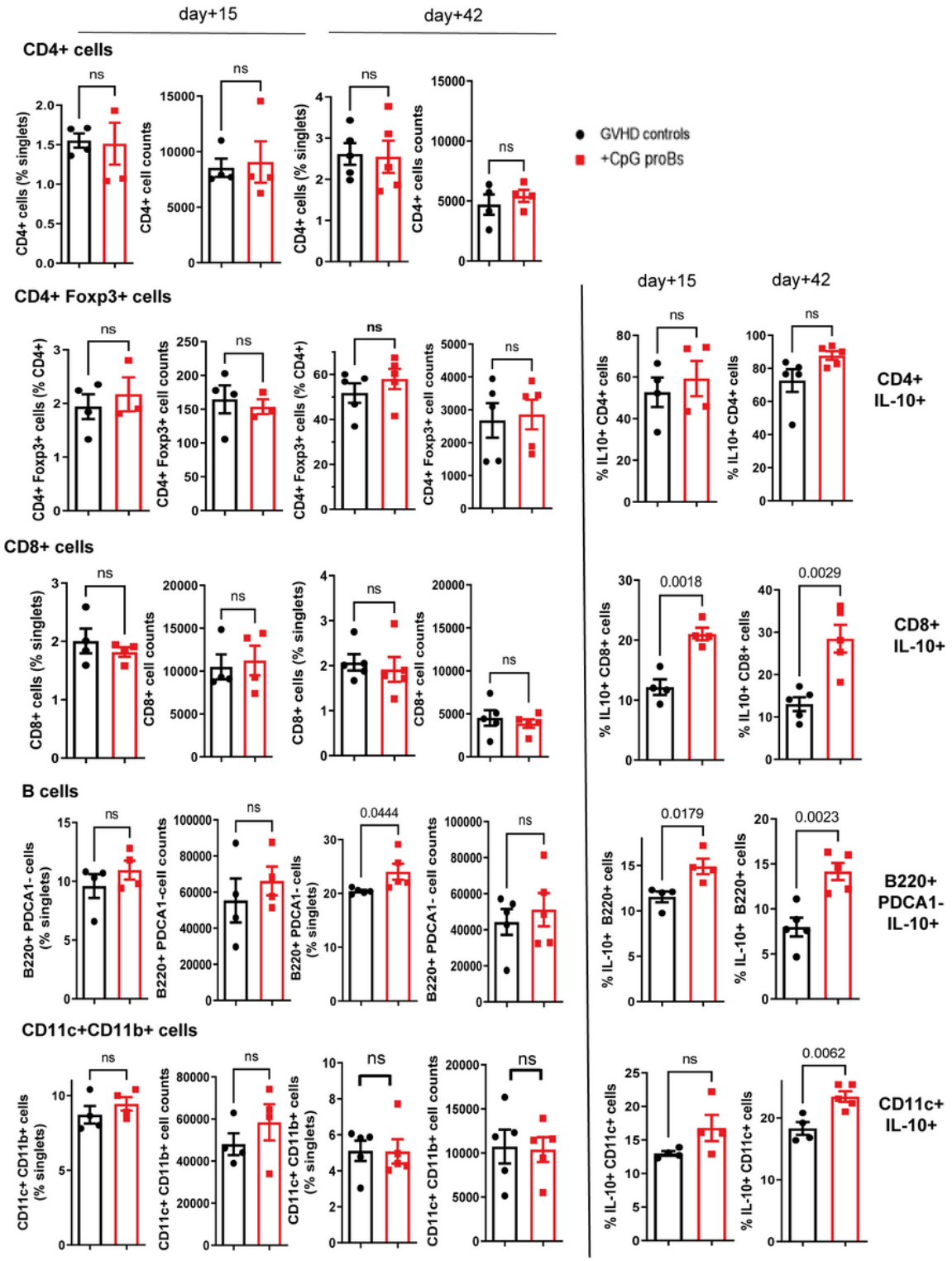

Figure 7

Flow cytometry analysis of skin infiltrates on day-15 and day-42 post-irradiation. CD4+, CD4+Foxp3+, CD8+, B220+PDCA-1- B and CD11c+CD11b+ dendritic cell percentages and cell counts are shown in GVHD controls (black) and CpG-proB recipients (red). IL-10-expressing fraction of CD4+, CD8+, B220+ and CD11c+ cells on day+15 and day+42 in the skin of GVHD controls (black) and CpG-proB recipients (red).

Results are expressed as means ± SEM for 5 mice per group. Statistical analysis was performed with unpaired Student's t-test, ns, non significant. p values as indicated.

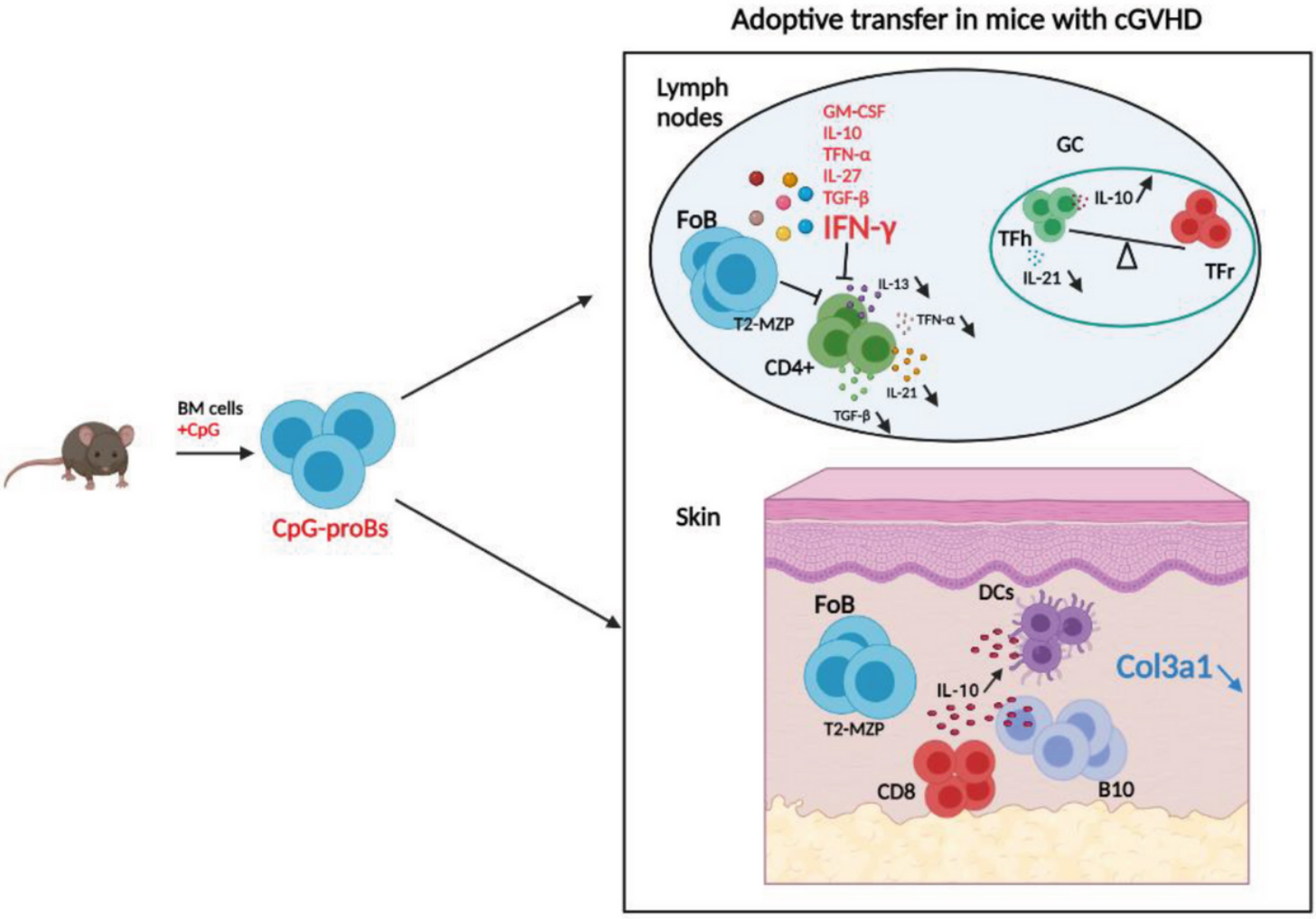

Figure 8

Graphical summary of the protective effects of CpG-proBs against sclerodermatous cGVHD. Adoptive transfer of CpG-proBs at the early phase of cGVHD alleviated disease symptoms, in particular skin fibrosis. Following their migration into lymph nodes and skin, these progenitors produced many cytokines but depended on IFN-γ production for their protective effect. CpG-proB transfer reduced the CD4+ T-cell production of profibrotic cytokines TGF-β, IL-21 and IL-13 and enhanced the Tfr/Tfh T-cell ratio in lymph nodes. They also promoted the accumulation of IL-10-producing B-cells, dendritic cells and CD8+ T-cells in the skin.

Supplementary Files

This is a list of supplementary files associated with this preprint. Click to download.

- FigureSupp1.pptx

- FigureSupp2.pdf
- FigureSupp3.pdf
- FigureSupp4.pdf